# Cracking phase diagram for the dynamics of an enzyme

Hao Qu,[1] Jonathan Landy,[2] and Giovanni Zocchi[1,*]

[1]*Department of Physics and Astronomy, University of California, Los Angeles, Los Angeles, California 90095-1547, USA*

[2]*Materials Department, University of California, Santa Barbara, Santa Barbara, California 93106-5121, USA*

(Received 29 March 2012; published 24 October 2012)

We measure the ensemble averaged deformation of an enzyme for an oscillating applied force. From the low frequency divergence of the mechanical susceptibility for the hinge motion of guanylate kinase we obtain a nonequilibrium phase diagram in the frequency-force plane. A phase line separates linear elasticity dynamics from softer (viscoelastic) dynamics. The hinge motion corresponds to crossing this phase line (not to a soft linear elastic mode). The phase line is dramatically shifted in the closed state compared to the open state of the enzyme.

DOI: 10.1103/PhysRevE.86.041915 PACS number(s): 87.15.Zg, 87.15.hp

## I. INTRODUCTION

Virtually all enzymes couple catalysis to conformational motion. Evident in motor proteins, mechanochemical coupling is also the basis for substrate specificity [1,2] and activity regulation [3–5] in these molecular machines. Conformational changes coupled to catalysis are often large, with amplitudes of $\sim 1$ nm compared to an overall size of the enzyme of $\sim 5$ nm. The folded protein being a solid, these huge strains pose an interesting question about the nature of conformational dynamics and the associated material properties of the system. Surely this motion is not within the linear elasticity regime, and a specific nonlinear mechanism for these transitions, called "cracking," was proposed some years ago [6,7]. Cracking connects initial and final states through a local melting and refolding event. Translated into stress-strain relations, this should give rise to an interesting dynamics. Here we measure directly the stress-strain relations for the hinge motion of the enzyme guanylate kinase (GK), a molecule quite similar to the enzyme considered in [6,7]. Specifically, we report comparative nanorheology [8] measurements on the open (no substrate) and closed (with the substrate GMP) forms of the enzyme and find that while the linear elasticity regime is almost the same, the nonlinear behavior, or what we have called the viscoelastic regime [9,10] is dramatically different in the two cases. A phase diagram in the frequency-force plane maps out regions of linear elastic vs softer (viscoelastic) dynamics. The existence of this phase line may be a universal feature of the dynamics of enzymes.

## II. RESULTS

The experimental system (Fig. 1) is described in detail in [8–10]. Briefly, the enzyme under study (GK from *Mycobacterium tuberculosis*, a $\sim 4$ nm size, $\sim 200$ amino acid globular protein which catalyzes the transfer of a phosphate group from ATP to GMP) tethers 20 nm size gold nanoparticles (GNPs) to an optically transparent ($\sim 30$ nm thick) gold layer evaporated on a glass slide. The protein is attached to the gold surfaces through cysteines introduced by mutagenesis on the two lobes of the structure. The "hinge motion" [11] which transforms the structure from the open to the closed form (Fig. 2) upon binding the substrate GMP—a classic example of induced fit [1]—roughly corresponds to moving the two cysteines by 1 nm towards each other. At each enzymatic cycle the molecule presumably performs this motion, though the pathway cannot be deterministic.

In the experiments, we drive the GNPs (which are negatively charged due to surface bound charged polymers) with an oscillating electric field generated by applying an ac voltage ($\sim 500$ mV rms, in the frequency range 10 Hz–10 kHz) between the gold layer and a similar upper electrode which forms the top of the $\sim 200$ $\mu$m thick sample cell. This chamber is filled with a threefold diluted saline-sodium citrate buffer solution (SSC/3), giving an ionic strength of $\sim 50$ mM and a corresponding Debye length of $\sim 1$ nm. The amplitude of oscillation of the GNPs is measured by evanescent wave scattering [12] in a phase locked loop. This oscillation is collective, whereas the thermal motion of each individual GNP is independent; by averaging over many GNPs (there are $\sim 10^8$ GNPs in the field of view of the lens which collects the scattered light) it is possible to measure oscillation amplitudes of a fraction of 1 Å, whereas the amplitude of thermal motion of an individual GNP is several nanometers [10]. This extraordinary resolution allowed us to measure the mechanical response function of the protein as it transits from the linear elasticity regime (at low forcing and high frequency) to a regime (at high forcing and low frequency) which we called viscoelastic [9,10]. In these experiments, the force on the GNPs is not calibrated, however we know that it is proportional to the applied voltage in the range of the experiments from control experiments using single-strand DNA molecules as tethers; these controls are published in [9]. Similarly, we know that the force on the GNPs is independent of frequency, from experiments at low force, where we expect elastic behavior and observe indeed a flat response vs frequency [8,9]. At fixed amplitude $F_0$ of the forcing, the amplitude of the response $|z|$ vs frequency $\nu$ is constant at high frequency (the response of a spring) and diverges at low frequency (the response of a viscous fluid) [9]. At fixed frequency $\nu$, $|z|$ vs $F_0$ is piecewise linear, the protein softening beyond a yield strain which defines the extent of the linear elasticity regime [10].

Here we start by presenting more detailed measurements of the low frequency divergence of the response function, shown in Fig. 3(a). The graph shows the amplitude of oscillation (in Å) vs driving frequency $\nu$ obtained for the same sample and

*zocchi@physics.ucla.edu

 

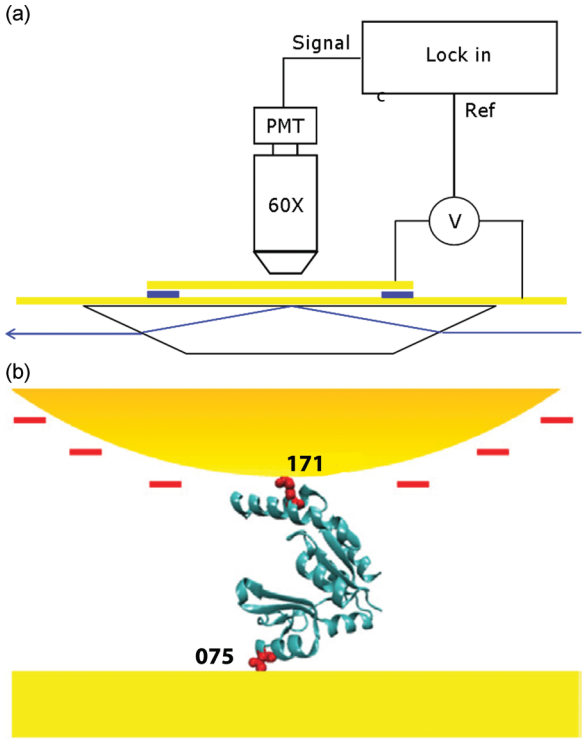


FIG. 1. (Color online) The experimental system. (a) The sample chamber with ac electric field and synchronous evanescent wave scattering optical measurement of deformation. (b) The geometry of the enzyme GK tethering a GNP to the gold coated slide. The attachment points (residues mutated to cysteines at positions 171 and 75) are shown on the structure. The enzyme and the GNP are drawn approximately to scale.

different amplitudes of the driving voltage. The high frequency response is flat, the plateau value being proportional to the driving force $F_0$ within experimental uncertainty. This is the behavior of a spring. Measurements of this plateau in a wider frequency range are reported in [8,9]. For $\nu \to 0$ the response diverges as $1/\nu$, as shown by the solid lines. This is the behavior of a viscous fluid. The functional form we use to fit the data of Fig. 3(a) reflects this behavior and is discussed below. It defines a corner frequency $\omega_1$ below which the system "flows." This corner frequency shifts to higher values for increasing

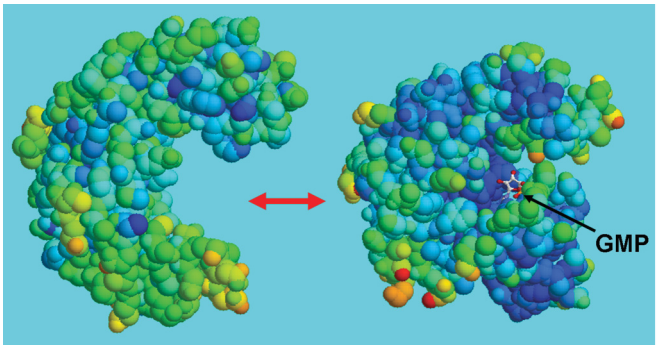


FIG. 2. (Color online) The open to closed conformational change (hinge motion) of (yeast) GK. Shown are the crystallographic structures of the enzyme with and without GMP bound (PDB structures 1EX7, 1EX6).

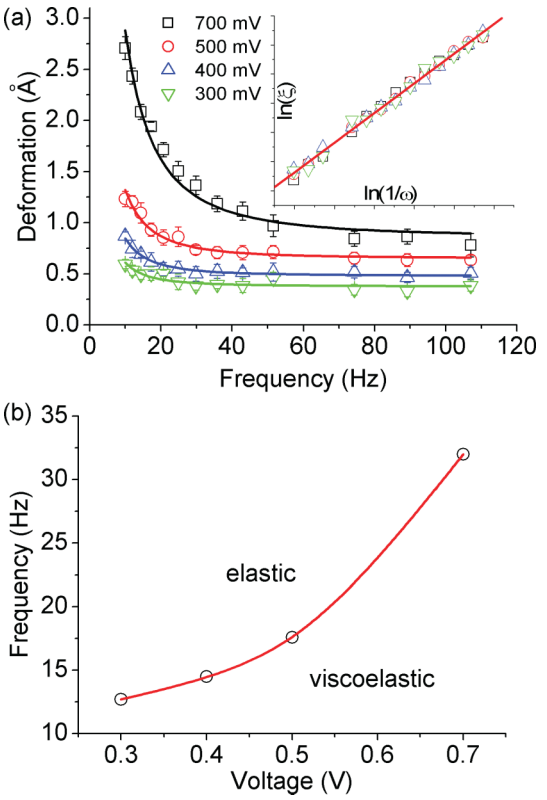


FIG. 3. (Color online) (a) Ensemble averaged amplitude of the deformation $|z|$ vs frequency $\nu$ for different driving voltages, showing the low frequency divergence of the susceptibility. The lines are fits to the data using Eq. (4). The error bars represent standard deviations ($\pm$SD) over five measurements (on the same sample). The inset is a plot of $\ln(\xi) = \ln[|z|/(A\sqrt{1+(\omega/\omega_1)^2})]$ vs $\ln(1/\omega)$ for the same data, showing the data collapse obtained using Eq. (4). The best linear fit has a slope of 1. (b) The phase diagram of the viscoelastic transition, obtained by plotting the corner frequency $\omega_1$ obtained from (a) vs the voltage $V$. The line, which is a fit using Eq. (7), separates linear elastic from softer (viscoelastic) dynamics.

amplitude of the forcing. This is shown in Fig. 3(b), where we plot the corner frequency $\omega_1$ vs applied voltage $V$. The line through the points (which we discuss later) separates the $\omega$-$V$ plane into two regions: one where we observe linear elasticity ("elastic"), and the other where we observe softening of the protein ("viscoelastic"). The transition between the two regimes is sharp when the response amplitude is plotted against the applied force [10], Fig. 4, so Fig. 3(b) constitutes a phase diagram of the dynamical behavior of the protein.

We may similarly probe the dynamics of the closed state. We add 1 mM GMP, which is saturating concentration (the binding constant for GMP is $K_G \approx 200\ \mu$M [5]). Figure 5 shows the response of the enzyme in the "open" state (in the absence of GMP: squares) and in the "closed" state (with GMP bound: circles), for the same sample. The high frequency plateau, which defines the linear elasticity stiffness, changes very little; from accurate measurements in a wider frequency range we know in fact that with GMP bound this stiffness is increased by about 30% [8]. But the low frequency divergence is dramatically different, the open state being "softer" in this regime than the closed state. In short, the so-called hinge

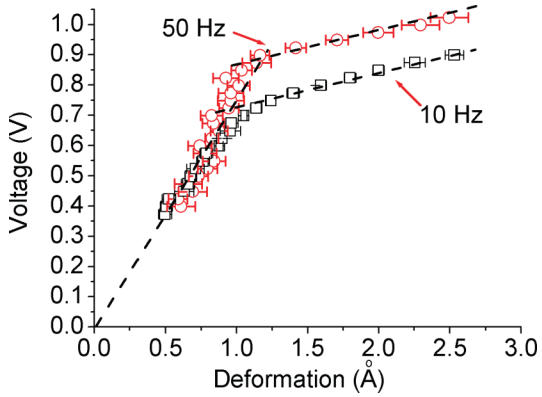


FIG. 4. (Color online) Forcing amplitude vs deformation at fixed frequency; circles: $\nu = 10$ Hz; squares: $\nu = 50$ Hz. The linear elasticity regime is extended at the higher frequency. The transition to the soft (viscoelastic) dynamics is sharp.

motion displays indeed a "soft" dynamics, but not in the linear elasticity regime (i.e., no "soft mode"). Instead, it is the phase line between elastic and viscoelastic (or soft) dynamics which is displaced (towards higher frequencies) in the open state compared to the closed state. Finally, we remark that all measurements presented here are reversible and cannot be attributed to electrochemical effects, but must reflect the dynamics of the tethers.

We now summarize quantitatively these observations by means of a heuristic model of the ensemble averaged protein's mechanics which we introduced previously [9,10]. The basic observation is that the ensemble averaged deformation, measured in the experiments, shows elastic behavior at high frequency and viscous flow behavior at low frequency. This is called viscoelasticity, and is captured in its simplest form by the Maxwell model, which is a spring and dashpot in series [Fig. 6(b)]. The relation between force $f$ and displacement $z$ for this model is

$$\frac{dz}{dt} = \frac{1}{k}\frac{df}{dt} + \frac{1}{\gamma}f(t), \tag{1}$$

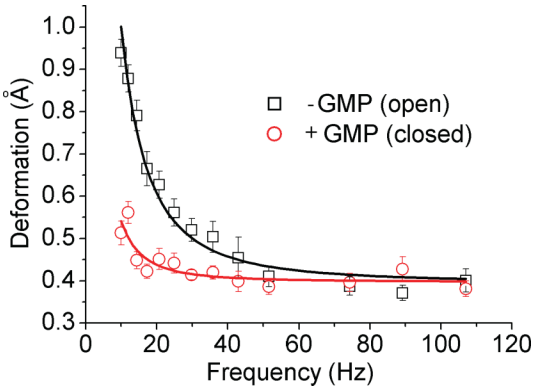


FIG. 5. (Color online) Deformation amplitude $|z|$ vs frequency $\nu$ for the same sample and driving voltage, in the presence (circles: closed state) and absence (squares: open state) of the substrate GMP. While the linear elasticity (large $\nu$) is essentially the same in the two cases, the low frequency behavior is dramatically different.

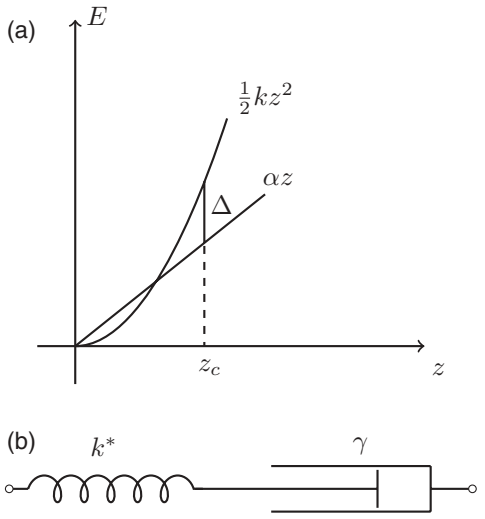


FIG. 6. (a) Sketch of a possible zero frequency free energy as a function of deformation $z$. The quadratic branch corresponds to linear elasticity and the linear branch gives rise to the soft (viscoelastic) dynamic states. Metastable states of energy $\Delta$ with respect to the ground state are accessible dynamically. (b) The simplest (Maxwell) model of viscoelasticity: a spring and dashpot in series.

where $k$ is the spring constant and $\gamma$ is the dissipation coefficient of the dashpot. In the experiment, this object is coupled to a GNP. The equation of motion of the GNP is

$$F(t) = f(t) + \gamma_0 \frac{dz}{dt}, \tag{2}$$

where $F$ is the force applied by the electric field. $\gamma_0$ is the hydrodynamic dissipation coefficient of the GNP, and inertial effects are negligible at the frequencies of interest. There is no thermal motion term in (1) or (2) because $z$ is an ensemble averaged quantity. This deterministic dynamics reproduces exactly the ensemble averaged dynamics of the corresponding Langevin equations, because the system is linear (see Supplemental Material in [10]). From (1) and (2), with an oscillating force $F = F_0 \sin(\omega t)$ one finds that the amplitude of the response is

$$|z| = \frac{F_0}{(\gamma + \gamma_0)\omega}\sqrt{\frac{1 + (\omega/\omega_1)^2}{1 + (\omega/\omega_2)^2}}, \tag{3}$$

where $\omega_1 = k^*/\gamma$ is the corner frequency of the viscoelastic element and $\omega_2 = k^*(\gamma + \gamma_0)/(\gamma\gamma_0)$. For $\gamma \gg \gamma_0$, which is the case for this setup [9], $\omega_2 \gg \omega_1$ and at frequencies $\omega \ll \omega_2$ (the regime we explore here) this response simplifies to $|z| \approx [F_0/(\gamma\omega)]\sqrt{1 + (\omega/\omega_1)^2}$. This describes very well the frequency dependence at fixed force $F_0$ [Fig. 3(a)]. With this motivation, we fit the data of Fig. 3(a) with the form

$$|z| = \frac{A}{\omega}\sqrt{1 + \left(\frac{\omega}{\omega_1}\right)^2}, \tag{4}$$

and determine for each data set the parameters $A$ and $\omega_1$. In the inset of Fig. 3(a) we show the data collapse obtained by plotting $\ln \xi$ vs $\ln(1/\omega)$ (where $\xi = |z|/[A\sqrt{1 + (\omega/\omega_1)^2}]$), using these values of $A$ and $\omega_1$. The slope of the graph

is $1.02 \pm 0.02$ showing that the response function indeed diverges as $1/\omega$ for $\omega \to 0$. Figure 3(b) shows the values of the corner frequency $\omega_1$ [obtained from the fits of Fig. 3(a)] plotted against the driving voltage $F_0$. The relation $\omega_1 = \omega_1(F_0)$ defines a phase line in this diagram separating elastic from dissipative response. The existence of this phase line is a main new result in the mechanochemistry of enzymes.

We now calculate the shape of the phase line, which is a stretched exponential (i.e., $\log \nu$ increases faster than linearly with $V$). Noting that the yield deformation $z_c$ depends on frequency (Fig. 4), we assume that the dc elastic energy $E$ vs deformation $z$ of the protein has the qualitative behavior sketched in Fig. 6(a). The equilibrium states follow the lower of the two branches in Fig. 6(a). But there are also nonequilibrium (metastable) states—the higher of the two branches—which are accessible to the system dynamically. We assume this generic picture of a bifurcation (e.g., the energy diagram for the Euler buckling instability is similar) inspired by our measurements of the equilibrium bending elastic energy of another biopolymer, double-strand DNA [13]. Assume that for $\omega > 0$ the system can access the metastable states on the $z^2$ branch [Fig. 6(a)]. The lifetime $\tau$ of such a state is [see Fig. 6(a)]

$$\tau \propto \exp(-\Delta/T) = \exp\left[-\left(\tfrac{1}{2}kz_c^2 - \alpha z_c\right)/T\right], \qquad (5)$$

which yields the relation between $\omega$ and $z_c$:

$$\frac{1}{\omega} = \frac{1}{\omega_0}\exp\left[-\left(\frac{1}{2}kz_c^2 - \alpha z_c\right)\Big/T\right], \qquad (6)$$

and since $F_c = kz_c$, we obtain the frequency dependence of the critical force:

$$T\,\ln\left(\frac{\omega}{\omega_0}\right) = \frac{1}{2k}F_c^2 - \frac{\alpha}{k}F_c. \qquad (7)$$

Interpreting (7) as a relation between the corner frequency $\omega_1$ and $F_0$, we obtain the solid line in Fig. 3(b). Thus Fig. 3(b) represents a nonequilibrium phase diagram for the protein, the phase line separating regions in the frequency-force plane where the dynamical behavior is elastic/viscoelastic.

We may apply these ideas to the measurements of the response in the open and closed states. We fit the data of Fig. 5 with the form (4) and obtain the parameters $A_+ = 3.67 \pm 0.33$, $\nu_1^+ = 9.23 \pm 1.01$ with GMP (closed state, circles) and $A_- = 9.20 \pm 0.25$, $\nu_1^- = 23.29 \pm 1.29$ without GMP (open state, squares). We notice that $A_-/A_+ \approx \nu_1^-/\nu_1^+$. Within the viscoelastic model, $\nu_1 = k^*/(2\pi\gamma)$, $A = \text{const.}/\gamma$, and we can describe the data by saying that $\gamma$ is a factor 2.5 smaller in the open state compared to the closed state, while $k^*$ is the same. The phase line in Fig. 3(b) is displaced in the closed state compared to the open state.

## III. CONCLUSIONS

Through a set of nanomechanical measurements of extraordinary resolution on the "hinge motion" of the enzyme guanylate kinase we arrive at the following experimental picture. The system undergoes a sharp (Fig. 4) transition from linear elasticity to a softer ("viscoelastic") dynamics as a function of force and frequency. Specifically, the susceptibility $\chi(\omega) = |z|/F_0$ diverges as $1/\omega$ for $\omega \to 0$ and goes to a constant for $\omega \to \infty$. We give an experimental description of this transition in terms of how the susceptibility $\chi(\omega)$ depends on the force: $\chi = \chi(\omega, F_0)$ [Figs. 3(a) and 4]. Namely, we experimentally define a line in the $\omega$-$F_0$ (frequency-force) plane [Fig. 3(b)] which separates elastic from viscoelastic response. In the representation of Fig. 3(a), following one curve towards lower frequencies corresponds to moving downwards along a vertical line in the phase diagram of Fig. 3(b): At some point one crosses from the elastic into the viscoelastic (soft) regime. Similarly, in the representation of Fig. 4, which shows plots of the forcing amplitude $F_0$ vs response amplitude $|z|$ at fixed frequency $\nu$, moving along a curve for increasing $F_0$ corresponds to moving along a horizontal line in Fig. 3(b). Again one crosses from the elastic to the viscoelastic regime at a certain (frequency dependent) critical force. We give a simple argument for the shape of this phase line, and show that in the closed state it shifts to lower frequencies compared to the open state. The open state is "softer" than the closed state (Fig. 5), not because its linear elastic constant is smaller, but because it is easier to access the soft (viscoelastic) state. Therefore, the hinge motion has nothing to do with "soft modes" and everything to do with the viscoelastic transition [9]. From Fig. 4 it is also evident that most (90%) of the 1 nm amplitude functional conformational motion of GK happens in the viscoelastic regime.

The conclusions above are experimental, independent of assuming the viscoelastic dynamics (3). However, assuming for the ensemble averaged dynamics of the protein, the model (3) produces remarkably good fits to the data [inset of Fig. 3(a)]. In this interpretation, the shift of the phase line in the open compared to the closed state is due to the dependence of the parameter $\gamma$ on force (a nonlinear effect).

The linear viscoelastic model (1) describes very well the frequency dependence of the measurements at fixed force $F_0$ [Fig. 3(a)]. However it does not describe the force dependence, which is nonlinear (Fig. 4). A comprehensive mathematical description of the transition, and eventually a microscopic model, are tasks for future work.

Onuchic, Wolynes, and collaborators, using structure based coarse grained simulations [6,7], have arrived at a structural description of the kind of conformational motion probed in our experiment. This description involves localized melting and refolding to connect open and closed states [6]. Qualitatively, it seems to us that a molten "hinge" would flow and thus produce a susceptibility which diverges as $1/\omega$, so we think that their predicted scenario, which they called "cracking" [6], and our observed dynamics, which we called the "viscoelastic transition" [9], may be one and the same. In this case, this study establishes experimentally the ensemble averaged dynamics of cracking.

## ACKNOWLEDGMENTS

This work was supported by the UC Lab Research Program, by NSF Grant No. DMR-1006162, and by the US-Israel Binational Science Foundation under Grant No. 2010448.

[1] D. E. Koshland, Jr., Proc. Natl. Acad. Sci. USA **44**, 98 (1958).
[2] Y. Savir and T. Tlusty, PLoS ONE **2**, e468 (2007).
[3] J. Monod, J.-P. Changeux, and F. Jacob, J. Mol. Biol. **6**, 306 (1963).
[4] M. F. Perutz, Nature (London) **237**, 495 (1972).
[5] C.-Y. Tseng, A. Wang, and G. Zocchi, Europhys. Lett. **91**, 18005 (2010).
[6] P. C. Whitford, O. Miyashita, Y. Levy, and J. N. Onuchic, J. Mol. Biol. **366**, 1661 (2007).
[7] O. Miyashita, J. N. Onuchic, and P. G. Wolynes, Proc. Natl. Acad. Sci. USA **100**, 12570 (2003).
[8] Y. Wang and G. Zocchi, Phys. Rev. Lett. **105**, 238104 (2010).
[9] Y. Wang and G. Zocchi, Europhys. Lett. **96**, 18003 (2011).
[10] Y. Wang and G. Zocchi, PLoS ONE **6**, e28097 (2011).
[11] J. Blaszczyk, Y. Li, H. Yan, and X. Ji, J. Mol. Biol. **307**, 247 (2001).
[12] H. Jensenius and G. Zocchi, Phys. Rev. Lett. **79**, 5030 (1997).
[13] H. Qu and G. Zocchi, Europhys. Lett. **94**, 10803 (2011).